Acoustic spectroscopy of lithium niobate: Elastic and piezoelectric coefficients

Hirotsugu Ogi,[a)] Yasunori Kawasaki, and Masahiko Hirao
Graduate School of Engineering Science, Osaka University, Osaka 560-8531, Japan

Hassel Ledbetter
Los Alamos National Laboratory, Los Alamos, New Mexico 87545

We report simultaneous measurement of the complete set of elastic and piezoelectric coefficients of lithium niobate (LiNbO$_3$), which has trigonal crystal symmetry (3m point group) and thus six independent elastic-stiffness coefficients C_{ij}, four piezoelectric coefficients e_{ij}, and two dielectric coefficients κ_{ij}. We used a single specimen: an oriented rectangular parallelepiped about 5 mm in size. Our measurement method, acoustic spectroscopy, focuses on the crystal's macroscopic resonance frequencies and is sensitive to any property that affects those frequencies. We overcame the principal obstacle to precise measurements—mode misidentification—by using laser-Doppler interferometry to detect the displacement distribution on a vibrating surface. This approach yields unambiguous mode identification. We used 56 resonances ranging in frequency from 0.3 to 1.2 MHz and determined the C_{ij} and e_{ij} with known κ_{ij}. The ten unknowns always converged to the same values even with unreasonable initial guesses. The C_{ij} uncertainty averages 0.09% for the diagonal C_{ij}. The e_{ij} uncertainty averages 5%. All our coefficients fall within the (surprisingly wide) error limits of previous (conventional) measurements. © *2002 American Institute of Physics.*
[DOI: 10.1063/1.1497702]

I. INTRODUCTION

Not occurring naturally, all crystals of lithium niobate are cultured. Its ferroelectricity was discovered in 1949.[1] Its crystal structure and physical properties received intense study at Bell Laboratories.[2–6]

Today, lithium niobate finds wide use as an electro-optical material. Its superior piezoelectric performance makes it a frequent replacement for quartz. As described by Weis and Gaylord,[7] lithium niobate enjoys a wide range of device applications that exploit its favorable elastic, piezo-electric, dielectric, acousto-optical, electro-optic, pyroelec-tric, photoelastic, and photovoltaic properties.

Crystals with 3m point-group symmetry show six inde-pendent elastic-stiffness coefficients (in contracted notation)[8]

$$[C_{ij}] = \begin{bmatrix} C_{11} & C_{12} & C_{13} & C_{14} & 0 & 0 \\ C_{12} & C_{11} & C_{13} & -C_{14} & 0 & 0 \\ C_{13} & C_{13} & C_{33} & 0 & 0 & 0 \\ C_{14} & -C_{14} & 0 & C_{44} & 0 & 0 \\ 0 & 0 & 0 & 0 & C_{44} & C_{14} \\ 0 & 0 & 0 & 0 & C_{14} & C_{66} \end{bmatrix}$$
$$(i,j = 1,2,..,6). \qquad (1)$$

Here, $C_{66} = (C_{11} - C_{12})/2$. They show four independent pi-ezoelectric coefficients[9]

$$[e_{ij}] = \begin{bmatrix} 0 & 0 & 0 & 0 & e_{15} & -e_{22} \\ -e_{22} & e_{22} & 0 & e_{15} & 0 & 0 \\ e_{31} & e_{31} & e_{33} & 0 & 0 & 0 \end{bmatrix}$$
$$(i = 1,2,3; \;\; j = 1,2,..,6). \qquad (2)$$

And, they show two independent dielectric coefficients[10]

$$[\kappa_{ij}] = \begin{bmatrix} \kappa_{11} & 0 & 0 \\ 0 & \kappa_{11} & 0 \\ 0 & 0 & \kappa_{33} \end{bmatrix} \quad (i,j = 1,2,3). \qquad (3)$$

Measuring the ten independent coefficients C_{ij} and e_{ij} presents a formidable task. As an example of previous stud-ies, we cite Smith and Welsh,[11] who showed that a complete set of coefficients could be obtained from ultrasonic phase-velocity measurements coupled with low-frequency capaci-tance measurements for the dielectric coefficients. These au-thors emphasize that this approach sometimes fails and then one must measure the electromechanical coupling factor and the natural frequencies of resonating bars. Of the ten coeffi-cients, only six result from direct measurements. Their laby-rinthine set of equations emphasizes the need for many mea-surements on many crystals in many orientations.

Here, we propose a method that yields all ten elastic and piezoelectric coefficients with a single frequency sweep on a single monocrystal. This approach was suggested by Dunn, Ledbetter, and Heyliger,[12] who showed that for lithium nio-bate large differences exist between resonance frequencies predicted by an elastic model and a dielectric–piezoelectric

---

a)Electronic mail: ogi@me.es.osaka-u.ac.jp

2451

model. By measuring resonance frequencies very accurately, the elastic and piezoelectric coefficients should be obtainable.

Our measurement method uses acoustic spectroscopy, often called resonance-ultrasound spectroscopy.[13–15] Our main improvement over previous measurement protocols was to use laser-Doppler interferometry to determine the displacement figure for each resonance, thus to identify unambiguously each resonance mode.

II. MEASUREMENTS

A. Crystal

From Z. Li (then at Argonne National Laboratory), we obtained an oriented monocrystal measuring 5.039 mm by 5.070 mm by 4.973 mm. Laue x-ray diffraction confirmed orientations within the measurement uncertainty of $1°$. The three sets of orthogonal faces were perpendicular to $[10\bar{1}0]$, $[\bar{1}2\bar{1}0]$, and $[0001]$ directions, along which we take the x_1, x_2, and x_3 axes, respectively. Using Archimedes's method and distilled water as a standard, we found a mass density $\rho = 4.636$ g/cm^3. From handbooks one finds $c = 13.856$ Å, $a = 5.147$ Å, and $\rho = 4.633$ g/cm^3, essentially identical with our measured density. The $[0001]$ direction constitutes a threefold rotation axis, which contains three mirror planes, one perpendicular to $[10\bar{1}0]$ in the standard setting. Within the $x_1 - x_2$ plane, all physical properties are isotropic (transverse isotropy), thus $C_{22} = C_{11}$, $e_{24} = e_{15}$, $\kappa_{22} = \kappa_{11}$, and so on.

B. Method

Acoustic spectroscopy,[13–15] measures the macroscopic resonance frequencies of a simple-shape specimen. Usually, one uses this method to determine the elastic-stiffness coefficients. However, one can use it to determine any property coupled to the macroscopic resonance frequencies. These include:

   (1) shape;
   (2) dimensions;
   (3) mass or mass density;
   (4) elastic stiffnesses; and
   (5) orientation.

Thus, the resonance spectrum represents a "fingerprint" of many interconnected properties. If the specimen is piezoelectric, then other properties enter:

   (6) piezoelectric coefficients and
   (7) dielectric coefficients.

In general, contributions of the last two properties to the macroscopic resonance frequencies are much smaller than those of the elastic stiffnesses, and precise measurements of the resonance frequencies are required to deduce them. Most acoustic-spectroscopy measurements sandwiched the specimen corners between two transducers for the acoustic transduction, which restrains the specimen's displacements and raises the resonance frequencies from those at *free* vibrations. Hence, we use a piezoelectric tripod consisting of two pinducers for generation and detection of vibration, and one just for support (Fig. 1). The specimen is put on the piezo-
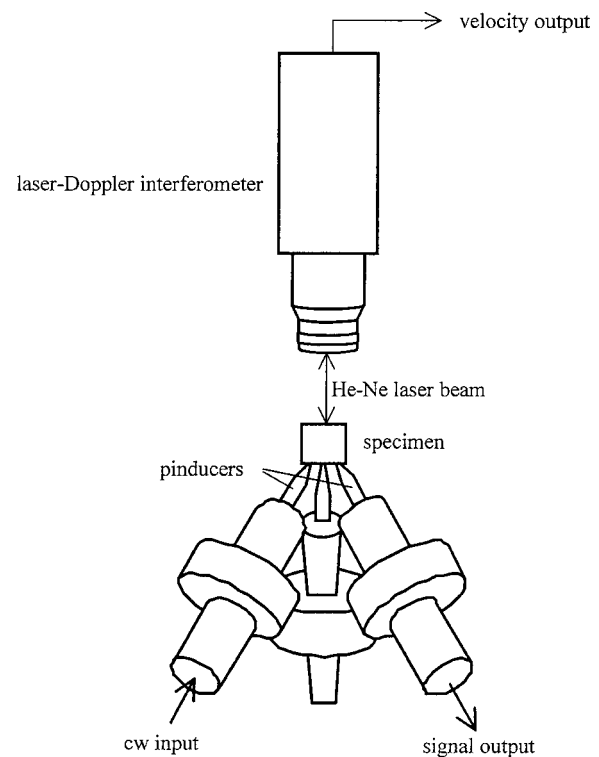

FIG. 1. Measurement setup showing piezoelectric tripod supporting a parallelepiped-shape specimen whose x_3-axis surface displacements were detected by a laser-Doppler interferometer.

electric tripod, without external forces except for its own weight. Contacts between the specimen and pinducers are therefore weak and stable, ensuring high reproducibility of the resonance-frequency measurements. We kept the specimen temperature at 30 ± 0.02 °C so that the reproducibility among completely independent measurements was better than 10^{-5}.

Acoustic-microscopy disadvantages include the need for a well-shaped specimen and the mode-misidentification problem. The latter has not been overcome. Successful determination of the material's properties requires finding exact correspondence between the observed and calculated resonance modes, that is, mode identification. If this is wrong, the resultant properties are physically meaningless. However, it has never been straightforward because measured resonance spectrum contains a large number of resonance peaks, providing no mode information. On the other hand, the calculation can tell the resonance modes. Then, one has to know beforehand the material's properties close to the true values to correctly compare the measurements with the calculations, otherwise mode misidentification easily occurs.

For correct mode identification, we used a laser-Doppler interferometer as shown in Fig. 1 to scan the displacement on a surface. A He–Ne laser beam was focused on the specimen surface (focal diameter: 15 μm). The reflected beam enters the Doppler interferometer, which detects the normal component of the velocity at the focal point. The velocity is easily converted into the displacement because of harmonic oscillation. Because lithium niobate is a transparent material, we deposited a 100 nm aluminum film on the (0001) surface

after completing the measurements of the resonance frequencies. The deposition shifted the resonance frequencies slightly, but the effect was so small that the mode correspondence between before and after deposition was unambiguous. Further details appear elsewhere.[16]

III. INVERSE CALCULATION

The governing equations expressing the interconnectivity of the elastic and electric properties are[17]

$$\sigma_i = C_{ij}S_j - \tilde{e}_{ik}E_k \quad (i,j=1,2,..,6; k=1,2,3), \quad (4)$$

$$D_i = e_{ij}S_j - \kappa_{ik}E_k \quad (i,k=1,2,3; j=1,2,..,6). \quad (5)$$

Here σ and S denote the stress and the engineering strain in contracted notation. E denotes electric field, D electric flux density, and $\tilde{e}_{ik} = e_{ki}$. The electric field can be divided into a rotational component and an irrotational component (or quasistatic field). In the megahertz-frequency region, the rotation component is negligible and the quasistatic electric field dominates,[18] which is expressed by the electric potential ϕ as

$$E_k = -\frac{\partial \phi}{\partial x_k}. \quad (6)$$

The simplest way to see the interconnectivity of these properties is to consider the equation of motion of plane waves traveling along the direction $\mathbf{l}=(l_1,l_2,l_3)$, that is, Christoffel equations[19]

$$\det[\mathbf{\Gamma} - \rho v^2 \mathbf{I}] = 0. \quad (7)$$

Here, ρ denotes mass density, v velocity of the plane wave, and $\mathbf{I}$ the identity matrix. For the elastic case, $\Gamma_{ij} = l_{ir}C_{rs}l_{sj}$ ($i,j=1,2,3; r,s=1,2,..,6$), where the matrix $[l_{ir}]$ is defined as

$$[l_{ir}] = \begin{bmatrix} l_1 & 0 & 0 & 0 & l_3 & l_2 \\ 0 & l_2 & 0 & l_3 & 0 & l_1 \\ 0 & 0 & l_3 & l_2 & l_1 & 0 \end{bmatrix}.$$

For the piezoelectric case,[20]

$$[\Gamma_{ij}] = l_{ir}\left[C_{rs} + \frac{e_{jr}l_j e_{is}l_i}{l_i \kappa_{ij} l_j}\right]l_{sj}. \quad (8)$$

Solving Eq. (7) yields three positive real eigenvalues ρv^2. Thus, the elastic stiffnesses are increased by the piezoelectric effect, that is, piezoelectric stiffening. The stiffness increases depend on the vibration mode. Equation (8) indicates that the stiffness modification is caused by the *combination* of the piezoelectric and dielectric coefficients, not by them independently. Therefore, with mechanical spectroscopy, one cannot determine the e_{ij} and κ_{ij} separately. However, the dielectric coefficients can be measured easily using low-frequency capacitance measurements.

To deduce the elastic and piezoelectric properties simultaneously, we perform an inverse calculation for the measured and calculated resonance frequencies following Ohno,[21] who presented a calculation method of the macroscopic resonance frequencies of a quartz rectangular parallelepiped crystal (32 point-group symmetry). He used linear combinations of the basis functions ψ consisting of the nor-

TABLE I. Four free-vibration groups of rectangular-parallelepiped oriented lithium niobate crystal classified by the degree of the Legendre polynomial bases.

Mode		l	$m+n$
A_g	u_1	O	E
	u_2	E	O
	u_3	E	O
	ϕ	E	O
A_u	u_1	E	E
	u_2	O	O
	u_3	O	O
	ϕ	O	O
B_g	u_1	E	O
	u_2	O	E
	u_3	O	E
	ϕ	O	E
B_u	u_1	O	O
	u_2	E	E
	u_3	E	E
	ϕ	E	E

malized Legendre polynomials to express approximately the actual displacements u_i and electric potential in the vibrating specimen, for which analytical solutions are unavailable

$$u_i(x_1,x_2,x_3) = \sum_k a_k^{(i)}\Psi_k^{(i)}(x_1,x_2,x_3), \quad (9)$$

$$\phi(x_1,x_2,x_3) = \sum_k a_k^{\phi}\Psi_k^{\phi}(x_1,x_2,x_3). \quad (10)$$

Here

$$\Psi_k(x_1,x_2,x_3) = \sqrt{\frac{8}{L_1 L_2 L_3}}\bar{P}_l(2x_1/L_1)$$

$$\times \bar{P}_m(2x_2/L_2)\bar{P}_n(2x_3/L_3). \quad (11)$$

$\bar{P}_l$ denotes the normalized Legendre polynomial of degree l and L_i denotes the edge length along the x_i axis of the rectangular parallelepiped. Lagrangian minimization with a Rayleigh–Ritz approach[13–15,21–25] determines the macroscopic resonance frequencies together with the associated sets of coefficients a_k. The rectangular-parallelepiped lithium niobate crystal has four vibration groups denoted by A_g, B_g, A_u, and B_u according to the deformation symmetry.[21,26] The elastic-piezoelectric interconnectivity leads to a corresponding symmetry of the electric potential as well, which differs from that of quartz. Because the symmetry of the deformation and electric potential is governed by
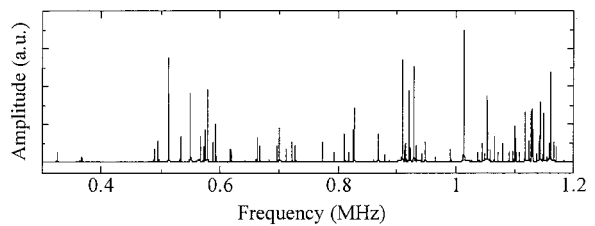

FIG. 2. Resonance spectrum. By an inverse calculation, the resonance frequencies yield the elastic and piezoelectric coefficients.
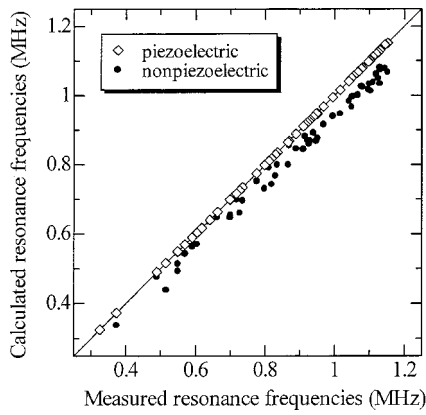
FIG. 3. Predicted vs measured resonance-peak frequencies. The correlation coefficient between the measurements and piezoelectric analysis is 0.999 99.

the degree of the Legendre polynomial (**E**ven or **O**dd), we can divide free vibrations into the four groups by evaluating the Legendre-polynomial degrees as shown in Table I. Choosing proper combinations of basis functions reduces calculation time. We included the Legendre polynomials
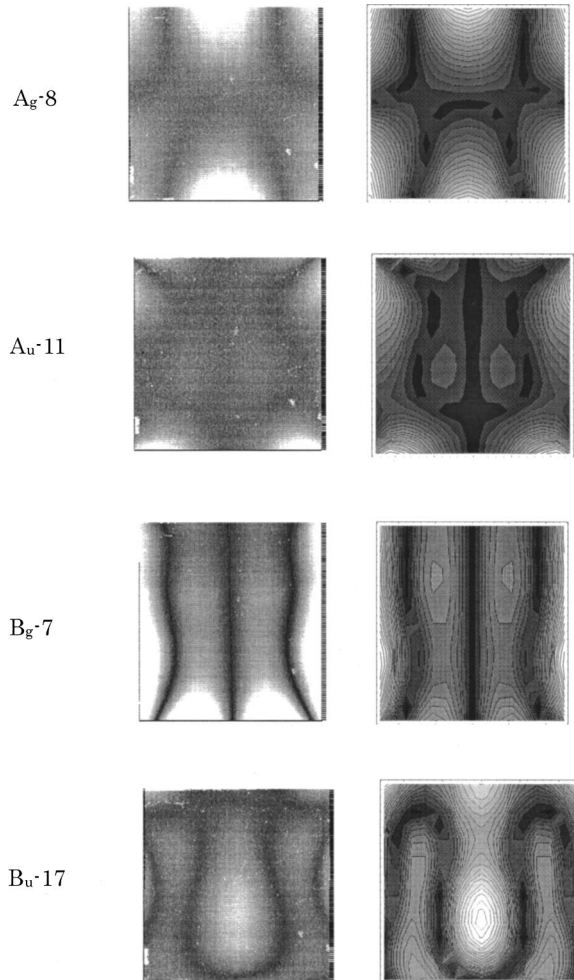

FIG. 4. Examples of measured (left) and computed (right) displacement figures along the x_3 axis on the z face of the crystal. Dark areas represent node lines. Typical displacement amplitude is one nm. The horizontal and vertical axes are along the x_1 and x_2 axes of the crystal, respectively.

TABLE II. Measured and calculated resonance frequencies of the lithium niobate crystal. The rms error between them is 0.09%.

Mode	f_m	f_c	Diff.(%)
A_u-1	0.325 351	0.325 222	−0.04
A_u-2	0.372 827	0.373 01	0.05
A_u-3	0.489 603	0.490 14	0.11
B_u-1	⋯	0.490 951	⋯
B_g-1	⋯	0.495 56	⋯
B_u-2	⋯	0.501 695	⋯
A_g-1	0.515 367	0.516 03	0.13
B_u-3	0.549 011	0.548 391	−0.11
B_g-2	0.548 699	0.549 46	0.14
A_g-2	⋯	0.567 101	⋯
A_u-4	0.568 932	0.569 531	0.11
A_g-3	⋯	0.573 198	⋯
B_u-4	⋯	0.573 993	⋯
B_g-3	⋯	0.580 393	⋯
A_g-4	0.589 799	0.589 625	−0.03
A_g-5	0.602 959	0.603 091	0.02
B_g-4	0.617 182	0.617 318	0.02
B_g-5	0.640 888	0.640 645	−0.04
A_g-6	0.66 302	0.663 178	0.02
A_g-7	⋯	0.671 538	⋯
B_u-5	⋯	0.6835	⋯
B_g-6	0.699 531	0.698 004	−0.22
A_u-5	0.698 426	0.699 204	0.11
B_u-6	0.716 54	0.716 383	−0.02
A_g-8	0.726 31	0.725 257	−0.15
A_u-6	0.734 215	0.734 688	0.06
A_u-7	0.774 928	0.774 832	−0.01
B_u-7	0.798 14	0.798 513	0.05
A_g-9	0.810 661	0.810 658	0
B_u-8	0.818 689	0.817 873	−0.1
B_u-9	0.829 478	0.829 465	0
A_u-8	0.835 145	0.83 499	−0.02
B_u-10	0.866 328	0.864 694	−0.19
A_u-9	0.868 907	0.868 434	−0.05
A_g-10	⋯	0.880 101	⋯
B_u-11	0.88 91	0.888 362	−0.08
B_g-7	0.910 393	0.910 837	0.05
A_u-10	0.916 148	0.915 92	−0.02
A_g-11	0.921 689	0.921 443	−0.03
B_g-8	0.926 254	0.925 603	−0.07
B_g-9	0.929 839	0.929 501	−0.04
B_g-10	0.938 723	0.938 218	−0.05
A_g-12	0.950 881	0.947 176	−0.39
B_u-12	0.947 714	0.947 873	0.02
A_g-13	0.968 434	0.967 707	−0.08
A_u-11	0.994 905	0.994 34	−0.06
A_u-12	1.016 239	1.015 45	−0.08
A_u-13	1.040 908	1.040 819	−0.01
B_g-11	1.049 125	1.049 673	0.05
B_u-13	1.049 631	1.050 541	0.09
A_g-14	1.054 975	1.056 065	0.1
B_u-14	1.066 507	1.066 003	−0.05
A_g-15	1.067 732	1.067 267	−0.04
B_g-12	1.076 394	1.077 097	0.07
A_u-14	1.080 066	1.080 05	0
A_g-16	1.097 344	1.097 328	0
A_u-15	1.100 799	1.101 092	0.03
B_u-15	1.103 102	1.102 319	−0.07
B_g-13	1.109 774	1.111 12	0.12
B_g-14	1.119 112	1.120 377	0.11
B_u-16	1.124 947	1.124 538	−0.04
A_u-16	1.130 25	1.130 521	0.02
A_g-17	1.130 514	1.131 832	0.12
B_g-15	1.131 718	1.133 518	0.16
B_g-16	⋯	1.145 2	⋯
B_u-17	1.14 4316	1.146 701	0.21
A_g-18	1.152 006	1.151 736	−0.02

TABLE III. Elastic coefficients (GPa), piezoelectric coefficients (C/m^2), and dielectric coefficients (10^{-12} F/m^2) of lithium niobate crystal; and average contributions of the coefficients to the resonance frequencies.

	Present	Damle (Ref. 29)	Warner and co-workers (Ref. 28)	Smith & Welsh (Ref. 11)	Dan'kov *et al.* (Ref. 27)	Kovacs *et al.* (Ref. 30)	Contributions[c] (%)
C_{11}	199.5 ± 0.20	203.1	203	203.0	199	198.4	17
C_{33}	235.2 ± 0.4	241.3	245	242.4	237.2	227.9	22
C_{44}	59.48 ± 0.04	64.6	60	59.5	60.1	59.65	28
C_{66}[a]	72.10 ± 0.01	75.1	75	72.8	72.6	71.84	45
C_{12}	55.27 ± 0.13	53	53	57.3	53.8	54.72	7.9
C_{13}	67.67 ± 0.26	74.2	75	75.2	71.4	65.13	10.8
C_{14}	8.7 ± 0.2	8.5	9	8.5	7.85	7.88	1.6
e_{15}	3.65 ± 0.03	⋯	3.7	3.76	3.61	3.69	10
e_{22}	2.39 ± 0.03	⋯	2.5	2.43	2.40	2.42	5.2
e_{31}	0.31 ± 0.04	⋯	0.2	0.23	0.28	0.30	0.16
e_{33}	1.72 ± 0.18	⋯	1.3	1.33	1.59	1.77	0.88
κ_{11}	398.9[b]	⋯	390	392	394	404	⋯
κ_{33}	-232.0[b]	⋯	257	247	231	233	⋯

[a]$C_{66} = (C_{11} - C_{12})/2$.
[b]Average of Refs. 27 and 30.
[c]The total departs from 100% because absolute values are shown.

with degree up to 12. The total number of the basis functions is 400–500 for each group in this case. We stopped the iterative calculation when the change of the rms error between the measured and calculated resonance frequencies became less than 5×10^{-6}. This is the criterion of the convergence of the inverse calculation.

We focus especially on the coefficients a_k. They reveal the displacement distribution on a specimen surface, which is a *signature* of an individual mode. Thus, comparison between the measured and computed displacement distributions guarantees correct mode identification.

IV. RESULTS

Figure 2 shows the measured resonance spectrum. For each mode, we fitted the Lorentzian function around the peak amplitude to determine the resonance frequency. Figure 3 shows measured resonance frequencies versus calculated by two models: piezoelectric and nonpiezoelectric. The difference between them permits determination of the piezoelectric coefficients. Figure 4 shows examples of the measured and computed displacement distributions on the x_3 surface. Excellent agreement permitted correct vibration-mode identification. A few modes showed poor agreement and we omitted them from the inverse calculation. Totally, we used 56 completely identified modes. Concerning the dielectric coefficients, we averaged the reported values and fixed them as $\kappa_{11} = 398.9 \times 10^{-12}$ and $\kappa_{33} = 232.0 \times 10^{-12}$ F/m^2. Table II compares the measurements and calculations after convergence. Their rms difference was 0.09%. The converged material coefficients are shown in Table III together with previously reported values.

V. DISCUSSION

First, we discuss the accuracy of our results. Four principal errors arise: (i) errors in the resonance-frequency measurement ($<0.001\%$), (ii) dimension errors ($<0.01\%$), (iii) crystal misorientation errors (less than $1°$), and (iv) calculation errors (0.09%). Thus, the maximum error lurks in the calculated resonance frequencies. Such a material coefficient that contributes little to the resonance frequencies compared with the error would not be determined with good accuracy. Table III shows the average contributions of the ten coefficients, $(q/f)(\partial f/\partial q)$, where q means C_{ij} or e_{ij}. The contribution of e_{31} is the smallest (0.16%), but it is still larger than the calculation uncertainty by a factor 1.8. Using their contributions and the calculation errors for each resonance mode, we estimated possible errors included in the result. These also appear in Table III. All our coefficients fall within the error limits of previous (conventional) measurements. The calculation error can be decreased by increasing the number of basis functions, but this drastically increases the computation time.

Second, we discuss the insensitivity of our results to the initial (guessed) values. The results given in Table III come from the initial set given by Dan'kov *et al.*[27] However, even with initial sets far away from the true values, the inverse calculation produced exactly the same results, owing to unambiguous mode identification. (The displacement-distribution patterns were hardly affected by the initial values as demonstrated in Ref. 16.) For example, use of the following unreasonable initial guesses, $C_{11} = 230$, $C_{33} = 200$, $C_{12} = 60$, $C_{13} = 80$, $C_{44} = 40$, and $C_{14} = 15$ GPa; $e_{15} = 5.0$, $e_{22} = 1.0$, $e_{31} = 0.1$, and $e_{33} = 3.0$ C/m^2, little affected the computed displacement patterns and resulted in coefficients that agreed with those in Table III within 0.02% for the C_{ij} and 0.2% for the e_{ij}.

Finally, we emphasize the importance of correct mode identification. Most studies with acoustic spectroscopy identified an observed mode by comparing only its frequency with calculations. In this procedure, mode misidentification certainly occurs unless *excellent* initial values are known in advance. Such misidentification, even for a few modes, affects highly the derived piezoelectric coefficients because of their weak contributions. For example, we made the inverse calculation using the initial set given by Warner, Onoe, and Coguin,[28] simplemindedly pairing the closest resonance frequencies between measurements and calculations without re-

ferring to the vibration patterns. Misidentification occurred for seven modes and the resulting C_{14}, e_{31}, and e_{33} disagreed with the correct values by 11%, 72%, and 25%, respectively, although other coefficients agreed within 3%. Thus, mode misidentification can be fatal when deducing a property that contributes little to the macroscopic vibrations.

VI. CONCLUSIONS

(1) We made the simultaneous determination of the six elastic coefficients and four piezoelectric coefficients of lithium niobate from a single specimen by using acoustic spectroscopy. We measured the macroscopic resonance frequencies with accuracy better than 0.001% and identified almost all observed (56) modes by measuring the displacement distributions on a surface using a laser-Doppler interferometry.

(2) Our values are consistent with those reported previously using conventional measurement methods where the values range widely.

(3) Our values are insensitive to the initial guessed set of coefficients, which are needed at the beginning of the inverse calculation. Even unreasonable guesses resulted in the same answers, owing to right mode identification. On the other hand, even good initial values failed to produce the correct answer with modes misidentified.

(4) Acoustic spectroscopy represents a viable alternative to conventional methods of measuring piezoelectric coefficients. Its principal advantages are simultaneous determination of the C_{ij} and e_{ij} on a single specimen. This provides enormous advantages for making measurements versus temperature, pressure, or stress. Also, measurements on specimens smaller than a millimeter would present few difficulties.

[1] B. Matthias and J. Remeika, Phys. Rev. **76**, 1886 (1949).
[2] K. Nassan, H. Levinstein, and G. Loiacono, J. Phys. Chem. Solids **27**, 983 (1966).
[3] K. Nassan, H. Levinstein, and G. Loiacono, J. Phys. Chem. Solids **27**, 989 (1966).
[4] S. Abrahams, J. Ready, and J. Bernstein, J. Phys. Chem. Solids **27**, 997 (1966).
[5] S. Abrahams, W. Hamilton, and J. Ready, J. Phys. Chem. Solids **27**, 1013 (1966).
[6] S. Abrahams, B. Buehler, W. Hamilton, and S. Laplace, J. Phys. Chem. Solids **34**, 521 (1973).
[7] R. Weis and T. Gaylord, Appl. Phys. A: Solids Surf. **37**, 191 (1985).
[8] J. Nye, *Physical Properties of Crystals* (Oxford, London, 1960), Table 9.
[9] Ref. 8 Table 8.
[10] Ref. 8 Table 5.
[11] R. Smith and F. Welsh, J. Appl. Phys. **42**, 2219 (1971).
[12] M. Dunn, H. Ledbetter, and P. Heyliger, in *Engineering Mechanics* (ASME, Washington DC, 1995), p. 758.
[13] O. Anderson, J. Acoust. Soc. Am. **91**, 2245 (1992).
[14] J. Maynard, Phys. Today **49**, 26 (1996).
[15] A. Migliori and J. Sarrao, *Resonant Ultrasound Spectroscopy* (Wiley-Interscience, New York, 1997).
[16] H. Ogi, K. Sato, T. Asada, and M. Hirao, J. Acoust. Soc. Am. (in press).
[17] B. A. Auld, *Acoustic Fields and Waves in Solids*, (Wiley-Interscience, New York, 1973), Vol. 1, p. 282.
[18] Ref. 17, p. 298.
[19] Ref. 17, p. 165.
[20] Ref. 17, p. 300.
[21] I. Ohno, Phys. Chem. Miner. **17**, 371 (1990).
[22] H. Demarest, J. Acoust. Soc. Am. **49**, 768 (1971).
[23] I. Ohno, J. Phys. Earth **24**, 355 (1976).
[24] H. Ledbetter, C. Fortunko, and P. Heyliger, J. Appl. Phys. **78**, 1542 (1995).
[25] H. Ogi, K. Takashima, H. Ledbetter, M. Dunn, G. Shimoike, M. Hirao, and P. Bowen, Acta Mater. **47**, 2787 (1999).
[26] E. Mochizuki, J. Phys. Earth **35**, 159 (1987).
[27] I. Dan'kov, E. Tokarev, G. Kudryahov, and K. Belobaev, Inorg. Mater. (Transl. of Neorg. Mater.) **19**, 1049 (1983).
[28] A. Warner, M. Onoe, and G. Coquin, J. Acoust. Soc. Am. **42**, 1223 (1967).
[29] R. Damle, J. Phys. D **25**, 1091 (1992).
[30] G. Kovacs, M. Anhorn, H. Engan, G. Visintini, and C. Ruppel, in Proceedings of the 1990 IEEE Ultrasonics Symposium, 1990, p. 435.